Matrix Chain Deformation in Reinforced Networks: a SANS Approach

S. Westermann,† M. Kreitschmann, W. Pyckhout-Hintzen,* and D. Richter

Forschungszentrum Jülich, Institut für Festkörperforschung, Postfach 1913, D-52425 Jülich, Germany

E. Straube

Martin-Luther-Universität Halle-Wittenberg, Fachbereich Physik, D-06099 Halle, Germany

B. Farago

Institute Laue Langevin, B.P. 156, F-38042 Grenoble Cedex 9, France

G. Goerigk

DESY/F41, Notkestrasse 85, D-22603 Hamburg, Germany

Received January 27, 1999; Revised Manuscript Received May 24, 1999

ABSTRACT: A small-angle neutron scattering (SANS) investigation of matrix chain deformation in an especially designed composite model system for a filled rubber−elastic network is presented. SANS experiments on the structure of polyisoprene homopolymer chains introduced into a well-microphase-separated triblock polyisoprene−polystyrene−polyisoprene (PI−PS−PI) system of the ABA type are reported. Use is made of the phase- and composition-matching techniques. The data are described in terms of the scattering behavior of the corresponding pure polyisoprene network at larger microscopic than macroscopic strains. The results confirm the model for the strain enhancement in reinforced networks and give the first direct microscopic insights into the mechanisms of reinforcement. A complementary small-angle X-ray scattering (SAXS) study yields all relevant geometrical parameters of the model filler and its detailed behavior under strain.

1. Introduction

It is a well-known fact that the filling of polymers and especially of rubbery networks with colloidal particles results in considerably improved mechanical properties. This phenomenon, which is commonly called reinforcement, is still not completely understood and has been the subject of numerous experimental investigations in the past.[1−7] As a consequence of the high technological importance and the need of new optimized materials nowadays, especially for processability purposes, a new drive toward a molecular understanding of the very complex behavior of reinforced networks could be observed lately.[8−15] Cross-links and chain entanglements fully determine the typical stress strain behavior of classical unfilled rubbers and for those a consistent theoretical approach is available.[16,17] For filled systems, however, additionally matrix−filler and filler−filler networking interactions as well as strain amplification effects of the matrix are expected to be important.[2,6,13,18−20] The filler−matrix interactions depend on the detailed structure of the surface. Through this surface activity, filler−filler interactions are also brought into play. Strain amplification, on the contrary, is a pure matrix property and describes the stiffening of the elastomeric matrix upon addition of hard fillers.[21,22] To unravel the underlying molecular processes quantitatively, it is essential to focus on all of these different mechanisms separately. This study will deal with strain amplification only. For this effect, the first evidences have been observed in the past only indirectly through the analysis of stress distribution patterns using birefringence and light-scattering methods.[23,24] In this paper, we present first direct experimental results on strain amplification on the chain level within the elastomer matrix in the presence of filler particles on a model system using the method of small-angle neutron scattering. We will look at filled elastomers as a composite system, made up by a soft rubber matrix and a rigid filler phase.

An improved understanding of stress−strain properties and especially of the microscopic deformation of elastic chains in ideal polymer networks in the absence of fillers is provided through analysis of the form factor $S(\vec{q},\Lambda)$ of a single chain under strain firmly embedded inside the polymer network.[25−32] Small-angle neutron scattering (SANS) is the only available bulk method to be pursued to date. Its wave vector range, covering molecular scales down to the segmental basis unit in polymers allows the ultimate investigation of both the chain deformation and chain fluctuations on all length scales of interest. Two-dimensional neutron scattering patterns obtained on networks at different strains were recently successfully interpreted in terms of a tube model.[28,33] This description led to the determination of the dynamic tube confinement parameter and confirmed its nonaffine deformation dependence.

Earlier studies of reinforcement established a relationship between the volume concentration of filler and the observed increased stiffness or Young modulus E in the linear region of tensile tests. Relative to the corresponding modulus of the unfilled network E_0, a reinforcement due to the hydrodynamic effect with

$$E = fE_0 \tag{1}$$

was defined.[1,7,21,22]

If it is further assumed that the stress is uniformly distributed, a mean amplified extension ratio $\bar{\lambda}$ may

† Present address: Goodyear Technical Center Luxembourg, L-7750 Colmar-Berg, Luxembourg.

10.1021/ma990112e CCC: $18.00
Published on Web 08/19/1999

then obtained from

$$\bar{\lambda} - 1 = f(\lambda - 1) \quad (2)$$

For typical loadings of fillers up to a volume fraction $\Phi \approx 0.35$, a Padé approximation of the expansion of f up to second order in the volume fraction Φ for a system of polydisperse undeformable spheres[34,35]

$$f = 1 + 2.5\Phi + 5.0\Phi^2 + O(\Phi^3) \approx 1 + \frac{2.5\Phi}{1 - 2\Phi} \quad (3)$$

turned out to be a suitable and theoretically founded expression for f. This is also supported by several empirical functions which are still popular in the literature and which vary only marginally by the factor of 2 in the denominator of eq 3. The first-order term is equivalent to the relative viscosity increase of a dilute suspension of spherical particles.[3,4] The second-order term on the other hand takes into account the elastic interparticle interaction and describes the influence of one matrix-coupled filler particle on the neighboring particles in the isotropically averaged stress field. Following the recommendations by Tobin,[21] retaining the same reinforcement factor for the matrix strain, stress−strain curves of typical carbon black[36] and silica[19] reinforced networks can be well described using the amplified extension ratio up to moderate deformation ratios.

To simulate ideal filler properties in a rubber−elastic medium in this investigation, a triblock copolymer of the type PI−PS−PI with a polystyrene middle block of $\Phi_{PS} = 0.18$ and two symmetric polyisoprene wings was tailor-made. Due to the repulsive interaction between the PS and PI blocks, this block copolymer undergoes a thermodynamically driven microphase separation; i.e., for this composition spherical PS domains are formed. The degree of the in situ filling is adjusted by simply blending the PI−PS−PI starlike micelles with a PI homopolymer matrix as the soft rubbery phase to give PS volume fractions of $\Phi_1 = 0.16$ and $\Phi_2 = 0.09$.

Unlike the thermoplastic block copolymer PS−PI−PS, our system has to be cross-linked to obtain a permanent network structure since the elastic, soft chains are only connected to one single domain. It is therefore expected that no additional cross-linking is introduced and the PI−PS−PI micelles formed by microphase separation can be considered as model fillers. Further, anionically synthesized PI shows no self-reinforcement due to crystallization which could mask the hydrodynamic strain amplification effect. Any difference in the elastic behavior can then be attributed to the physical presence of fillers.

The central purpose of our work—to investigate the matrix chain deformations by SANS in this system—requires matching off all scattering contributions of the PS filler domains and brushlike PI arms. This can be achieved using a blend of hydrogenous and deuterated homopolymers and PI parts of the copolymer that are statistically composed of hydrogenous and deuterated segments.[37,38] In addition, in a complementary SAXS experiment performed on the identical samples, all relevant geometrical information and the behavior of the PS domains under strain are revealed.

One single SANS investigation of a similar system under strain was reported earlier by Richards and Welsh.[8] They studied a phase matched PS−PI−PS mixture with deuterated and hydrogenated PI parts, and the radii of gyration of the deuterated PI blocks were analyzed using various network models. However, the overstrain due to the undeformable domains was neither explicitly investigated nor looked for.

We will show that a copolymer system of this type can be indeed a very valuable tool for a profound investigation of local deformation effects in reinforced networks and overstrains. The experimental data agree in detail with theoretical predictions based on a simple picture of filler and matrix developing strain relations.

2. Theoretical Modeling

SANS. A decade ago, the scattering theory of Benoit[39] was extended by Quan and Koberstein[37,38] with respect to the matching of partial structure factors to be applied to mixtures of homopolymers and copolymers. Use is made of two contrasting conditions: *composition matching* is achieved by means of two homopolymers so as to match the scattering length of a third component, and *phase matching* is applied to eliminate the scattering due to intrablock correlations in a block copolymer. An ideal situation arises if for a completely incompressible system a blend of homopolymers with equal chain length is diluted with a phase-matched copolymer or vice versa. For a complete review, we refer the reader to the original literature. As the final result for the scattering cross section of an incompressible blend of phase-matched copolymer with a blend of homopolymers, compositionally matched to this copolymer, we retain

$$\frac{d\Sigma}{d\Omega}(\vec{q},\Lambda) = (\Delta_{HH}{}^2 N_{HH} + \Delta_{HD}{}^2 N_{HD}) Z_H^2 S_D(\vec{q},\Lambda) \quad (4)$$

Here, N_i (i = HH, HD) is the number density of a homopolymer component, Z_H is the polymerization degree of the homopolymers, and $\Delta_i = b_i - b_{PS}$ (i = HH, HD) is the scattering length contrast between the homopolymers and both blocks of the copolymer which are phase-matched. The superstructure of the PS domains allows the easy identification of additional scattering contributions at nonideal contrast conditions. It is noted that the presence of the copolymer as third component does show up in the reduced scatterer densities N_{HH} and N_{HD} only. The internal contrast of the copolymer is zero as well as the interchain contrast with the homopolymers. Λ now represents the microscopic deformation tensor acting on the chain level with the components λ_μ ($\mu = x, y, z$).

In this case, the single chain form factor $S_D(\vec{q},\Lambda)$ can be extracted.

The microscopic matrix chain deformation in the reinforced network is evaluated using the tube model of rubber elasticity[17] which successfully describes the chain deformations of unfilled networks.[28,33] This model includes the topological constraints due to the other matrix chains in terms of an harmonic potential modeling thereby the range of localization in the tube picture. Recently, the strength of this model to predict properties was tested against more complicated than the uniaxial deformations used in most experiments.[40] The scattering function for a single labeled path in the matrix-network, $S(\vec{q})$, is

$$S_D(\vec{q},\Lambda) = 2\int_0^1 d\eta \int_0^\eta d\eta' \prod_\mu \exp\left(-(Q_\mu\lambda_\mu)^2(\eta-\eta') - Q_\mu^2(1-\lambda_\mu^2)\left\{\frac{d_\phi^2}{2\sqrt{6}R_g^2}\left(1-\exp\left(-\frac{\eta-\eta'}{\frac{d_\phi^2}{2\sqrt{6}R_g^2}}\right)\right)\right\}\right) \quad (5)$$

where R_g is the radius of gyration of the labeled path and $Q_\mu = q_\mu R_g$ is a component of the reduced scattering wave vector in the main axis system of the deformation tensor Λ acting on the chain level with the components λ_μ ($\mu = x, y, z$). $d_\phi^2 = d_\phi^2\lambda_\phi$ is the square of the tube diameter in scattering direction with the deformation ratio λ_ϕ in scattering direction, introduced as $\lambda_\phi^2 = \lambda^2\cos^2\phi + (1/\lambda)\sin^2\phi$. η and η' are dimensionless contour length coordinates extending over the labeled paths of the chains.

SAXS. Small-angle X-ray scattering enables us to determine the geometrical properties of our systems. The scattering contrast is only due to differences in the electron densities between polystyrene and polyisoprene domains. The exchange of hydrogen and deuterium isotopes is of no relevance, and the spherical PS domains can be regarded as the sources of scattering. The measured intensity is proportional to the product of the form factor of the spherical domains and the structure factor of the ensemble of all domains. The latter normally is a sensitive probe of ordering effects, typically modeled by a liquidlike Percus−Yevick structure factor[41] or a bcc latticelike structure factor.[42−44] The data were interpreted using both approaches since we are exclusively interested in the characteristic length scales and the deformation behavior of our system. It is beyond the scope of this paper to discriminate between the two different structural models.

In the PY approach polydisperse domains were assumed, corrected with a diffuse boundary σ as is usual for block copolymers. This boundary relates to the interfacial thickness. The structure factor in terms of the hard-sphere radius, R_{HS} and volume fraction η is well discussed in the literature and is omitted here.

Alternatively, also ordered bcc structures have been proposed in similar block copolymers.[42−44] The model previously introduced by Stuehn et al.[43,44] was adopted, in which the scattering intensities are the weighed sum of Bragg components $I_{Bragg}(q)$, appearing due to the regular periodic order. A diffuse term $I_{Diff}(q)$ with Debye−Waller correction is introduced and is related to the positional disorder of the micellar-like domains from their mean position in the bcc lattice. Besides average domain dimensions the model yields the lattice constant D which can be observed as a function of strain.

3. Experiments

Sample Preparation and Characterization. All polymers were prepared by anionic polymerization with *sec*-BuLi in evacuated and sealed glass reactors under high vacuum conditions at ambient temperatures. Solvents and monomers were purified to the standards required by anionic polymerization. For the triblock wings the monomers (H and D) were premixed. The phase matching condition is met for a triblock copolymer with polyisoprene arms statistically built up from 16 vol % deuterated and 84 vol % protonated monomers. A PI−PS diblock copolymer was synthesized in cyclohexane by subsequent polymerization of the isoprene monomer mixture followed by the styrene monomer. THF was added to facilitate the crossover reaction. The thus obtained diblock precursor was linked with dimethyldichlorosilane to obtain the symmetric PI−PS−PI triblock. Unreacted diblock material was eliminated by fractionation. The final PI−PS−PI triblock copolymer was obtained in a purity of (99 ± 2)%. The addition of THF after the polymerization of PI did not influence the microstructure, which is about 90% 1,4.

Molecular weights and weight distributions of the triblock copolymer and the PI and PI−PS precursors were measured independently by membrane osmometry (MO), low-angle laser light scattering (LALLS), and size exclusion chromatography (GPC), giving a total molecular weight of the whole triblock of 96 000, with $M_w/M_n = 1.02$. The styrene content of 18 vol % was confirmed by fluorescence spectroscopy against standard solutions. The molecular weight of the PI-arms of the triblock was determined to be $M_n = 42\,000$. The ODT of the block copolymer is estimated to be about 300 °C and is therefore higher than the cross-linking temperature. The homopolymer matrix consists of H−PI of $M_w = 90\,000$ and D-PI of $M_w = 102\,000$ with $M_w/M_n = 1.02$ ($N_H = N_D$). Absolute values for molecular weights are taken to be 5% accurate.

Statistical networks were prepared from the pure homopolymer mixture and of mixtures with 90% and 50% of the triblock-copolymer, to give total volume fractions of PS of $\Phi_1 = 0.16$ and $\Phi_2 = 0.09$, respectively. Composition matching is achieved by mixing 16 vol % deuterated and 84 vol % protonated homopolymers. The blend and the cross-linker, dicumylperoxide (DCP), were dissolved in THF (20% v/v) and transferred to a Teflon mold. The solvent was taken off in vacuum for several days and finally the system was cured in Ar atmosphere at 163 °C for 2 h to ensure complete decomposition of the peroxide. M_C, the mass of the elastic chains, was estimated from swelling experiments in cyclohexane. Cyclohexane is a good solvent for PI at room temperature, though only a Θ solvent for PS at 34°. However, for molecular weights of PS up to $M_w = 22\,000$ at 16 vol %, it experimentally dissolves PS very well at room temperature, and no precipitation can be observed after 1 week. This yields for the unfilled sample a molecular weight of 8880 ± 350, identical to 8530 ± 340 for the $\Phi_1 = 0.16$ and 8490 ± 340 for the $\Phi_2 = 0.09$ sample. These results were consistent with a complementary NMR analysis.[45] The average gel fraction was $w_{gel} = 0.962 \pm 0.004$. Therefore, the swelling method yields directly real elastic masses since the PS domains are also dissolved in the solvent, unlike in the (more difficult and model dependent) determination of the elastic moduli from stress−strain analyses. Consequently, no corrections for insoluble filler material which affects the swelling degree are necessary.

SANS. The small-angle neutron scattering experiment was performed using the D11 instrument at the ILL (Grenoble, France), with a neutron wavelength of $\lambda_N = 7.0$ Å and a wavelength spread $\Delta\lambda/\lambda$ of about 9%. Detector distances were 2.5 and 10 m, providing an experimental range of $0.006\ \text{Å}^{-1} \le q \le 0.13\ \text{Å}^{-1}$ in terms of the scattering vector $q = (4\pi/\lambda_N)\sin(\theta/2)$, θ being the scattering angle. The experiments in the strained state were performed in uniaxial extension with the macroscopic deformation tensor Λ_m having diagonal components λ, $1/\sqrt{\lambda}$, $1/\sqrt{\lambda}$. The extension ratio λ is defined as L/L_0, the actual (L) and initial length (L_0) of the sample within 5% accuracy from a grid of marks on the sample. The experimental lengths-to-width ratios upon straining were in absolute agreement with an affine sample deformation. The macroscopic sample deformation was checked by means of the measured sample transmission since the thickness changes with $1/\sqrt{\lambda}$ assuming incompressibility.

For the unfilled sample scattering intensities were recorded at macroscopic extension ratios $\lambda = \{1.00, 1.20, 1.40, 1.65\}$.

The network samples with filler contents of $\Phi_1 = 0.16$ and $\Phi_2 = 0.09$ were studied at comparable strains, $\lambda_{\Phi 1} = \{1.0, 1.4, 1.55, 1.7, 1.9\}$ and $\lambda_{\Phi 2} = \{1.0, 1.2, 1.4, 1.65\}$, respectively.

The raw data were normalized for monitor counts and corrected for background, empty beam, and detector sensitivity. The data were converted to absolute cross sections by

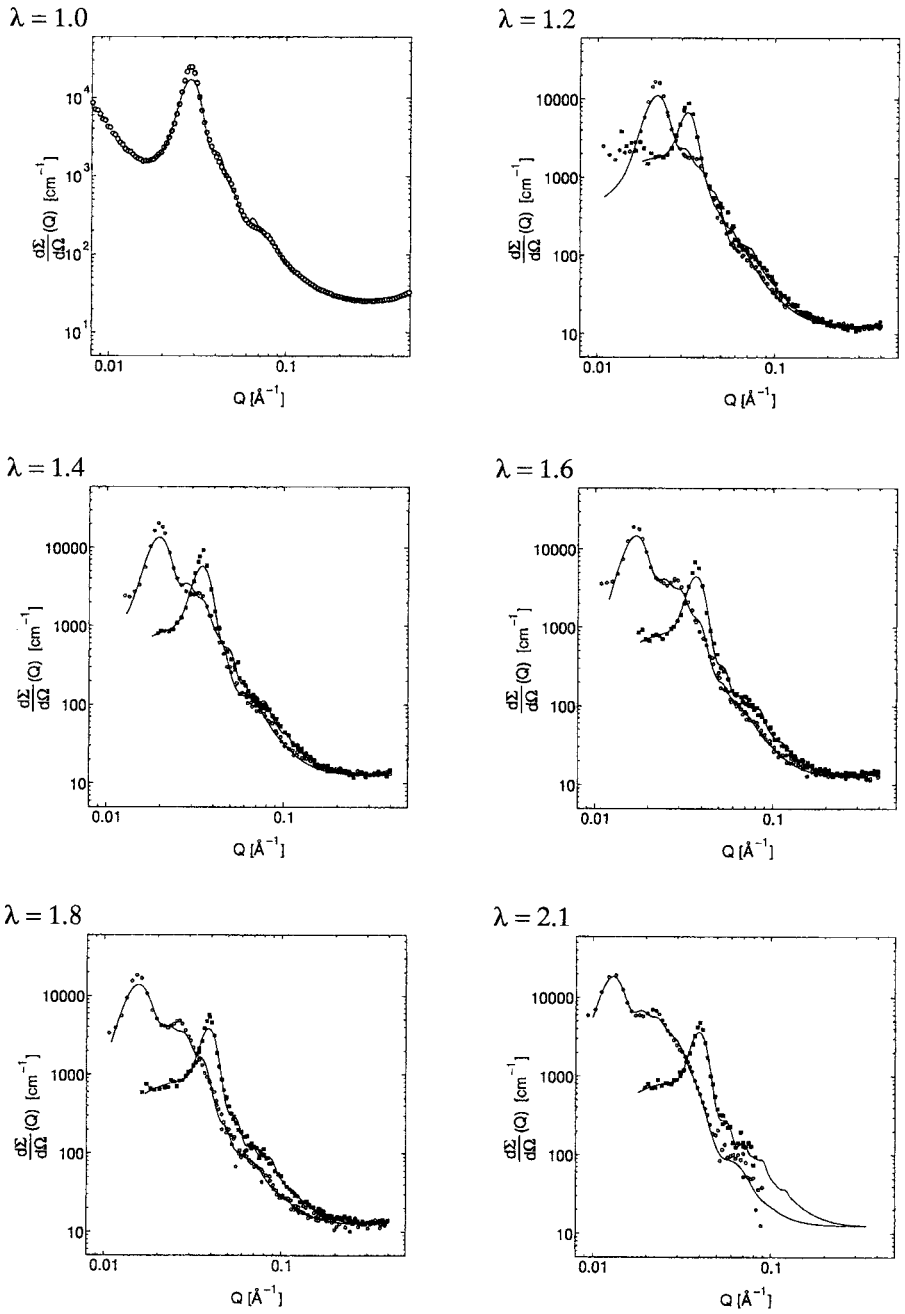

Figure 1. Fit results of the SAXS data using the bcc lattice model of Stuehn et al. The experimental data are well represented with average radius of the PS spheres of $R_m = 85$ Å and an affine displacement of the filler. Symbols: circles, parallel direction; squares, perpendicular direction.

means of the scattering of a water sample of 1 mm thickness. The incoherent scattering level was determined separately from a 100% protonated PI network sample of comparable cross-link density and a 100% protonated PS sample and subtracted weighed with its volume fraction.

In the case of isotropic scattering the data were radially averaged. The anisotropic data sets have been evaluated in the full 2D detector plane (64 × 64 channels) to retain the off-axis information on the complete scattering pattern. Axis data were less conclusive in this moderate strain regime and were omitted.

SAXS. The small-angle X-ray scattering experiments were performed at the Jusifa instrument at Desy/Hasylab (Hamburg, Germany) at a wavelength of $\lambda_X = 1.54$ Å. The accessible q range was $0.006\ \text{Å}^{-1} \le q \le 0.55\ \text{Å}^{-1}$. The network sample with a filler content of $\Phi_1 = 0.16$ was studied in the same manner as described for the SANS experiments at extension ratios $\lambda = \{1.2, 1.4, 1.6, 1.8, 2.1\}$. The data were corrected for absorption, background and detector sensitivity. The data were collected in 256 × 256 channels. Anisotropic spectra were interpolated along the main axes using a procedure provided at the instrument.

4. Results

4.1. SAXS. Figure 1 shows the obtained SAXS results for the Φ_1 network for different extension ratios. The solid lines correspond to the bcc lattice structure factor[43,44] and the average form factor of polydisperse spheres. For the isotropic network an average radius of the spheres of $R_m = 85 \pm 1$ Å and $\sigma_R/R_m = 0.145$ was obtained. The lattice constant was determined to be $D = 303 \pm 6$ Å with $\sigma_R/D = 0.144$. σ_i (i = R, D) are Gaussian widths of the distributions. The root mean-square displacement $u = 22 \pm 4$ Å agrees well with studies on comparable systems.[43] The volume fraction

Table 1

	Percus−Yevick			BCC lattice		
λ	R_m (Å)	σ_R (Å)	λ_{filler}	R_m (Å)	σ_R (Å)	λ_{filler}
1.0	83.0 ± 1.2	11.9	1.00	84.7 ± 0.9	12.3	1.00
1.2	87.5 ± 1.5	15.6	1.31 ± 0.05	89.1 ± 1.6	15.0	1.30 ± 0.05
1.4	87.9 ± 1.5	15.1	1.44 ± 0.05	88.6 ± 1.2	13.6	1.45 ± 0.05
1.6	91.2 ± 1.4	16.1	1.68 ± 0.05	91.4 ± 1.1	14.3	1.67 ± 0.05
1.8	90.7 ± 1.2	13.8	1.84 ± 0.05	91.8 ± 1.0	12.6	1.81 ± 0.05
2.1	93.2 ± 2.2	13.0	2.18 ± 0.05	93.4 ± 2.7	12.9	2.19 ± 0.05
$1.2^{-1/2}$	78.3 ± 1.3	11.8	0.87 ± 0.02	86.3 ± 1.2	13.7	0.88 ± 0.02
$1.4^{-1/2}$	75.2 ± 1.0	10.4	0.84 ± 0.02	79.4 ± 1.1	12.2	0.83 ± 0.02
$1.6^{-1/2}$	73.3 ± 1.4	10.9	0.77 ± 0.02	77.9 ± 1.1	11.6	0.77 ± 0.02
$1.8^{-1/2}$	73.4 ± 2.3	13.6	0.73 ± 0.02	75.7 ± 1.0	11.5	0.74 ± 0.02
$2.1^{-1/2}$	78.3 ± 4.1	16.5	0.71 ± 0.02	77.1 ± 2.1	12.3	0.73 ± 0.02

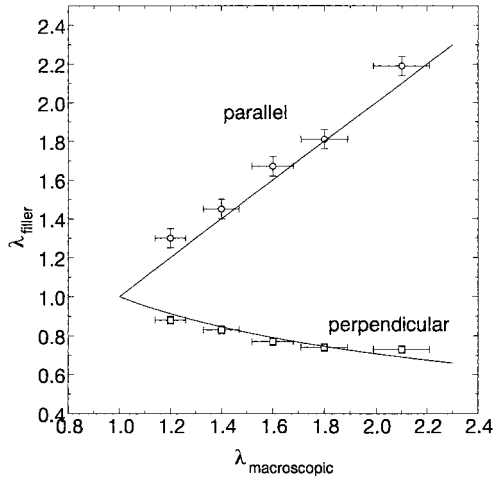

Figure 2. Correlation of the filler displacement Λ_{filler} as a function of the applied macroscopic sample strain as obtained from the bcc lattice model. The solid lines indicate the behavior predicted from an affine correlation.

of PS can be calculated to $\phi_{PS}^{bcc} = (8\pi/3)(R_m/D)^3 = 0.18 \pm 0.02$, which corroborates well with the chemical amount of PS of $\Phi_1 = 0.16$. The width of the diffuse boundary was determined by a Porod representation Iq^4 vs q in the large q region to be $\sigma = 4 \pm 3$ Å and was kept fixed during the refinement procedure. Its determination is error-prone in view of the rather limited q range. In particular, the correlation with the background subtraction, which is dominant in this q range, cannot be neglected. Therefore, the claimed accuracy is estimated by the range for σ for which no or hardly any observable differences in the fitting quality can be detected. The same principle was used for the quoted error bars in the other fitted parameters. For the stretched networks the straightforward transformation $D \rightarrow D(\Lambda = 1)$. Λ_{filler} was applied. $D(\Lambda = 1)$ was fixed to the isotropic value and the filler displacement Λ_{filler} was optimized in a nonlinear least-squares fitting process. Figure 1 shows the agreements from isotropic state to the maximum deformation of $\lambda_{||} = 2.1$. The width parameter σ_R exhibits no significant variations as a function of the applied strain. The results of the refinement are summarized in Table 1. It proves that the filler displacement, Λ_{filler}, is affinely correlated to the applied macroscopic extension ratio, Λ_{macr}, as shown in Figure 2.

The fits also indicate a small but systematic variation of the radius of the PS domains as a function of macroscopic strain, indicating a smaller than expected modulus of the PS domains, on which we will comment later.

Alternatively, the results using the hard-sphere structure factor in Percus−Yevick approximation and an averaged form factor of polydisperse spheres with a smeared boundary σ are shown in Figure 3. The same average radius of the spheres of $R_m = 83 \pm 2$ Å was derived. The hard sphere radius, $R_{HS} = 120 \pm 6$ Å leads to a hard sphere volume fraction $\eta_{HS} = 0.49 \pm 0.01$. For σ we have used the Porod result as above. We note that according to Hoover[46] at a critical $\eta = 0.494$ a transition to more ordered structures are favored.

On the basis of these isotropic results, scattering intensities for the anisotropic samples using the same transformation $R_{HS} \rightarrow R_{HS,\Lambda = 1}\Lambda_{\text{filler}}$ can be obtained. In contrast to the bcc-lattice structure factor discussed above, the structure factor peaks at low q are fitted quite well, whereas in the intermediate q region the deviations of the fits are slightly larger. The obtained parameters are enumerated in Table 1. The affine correlation of the filler displacement with macroscopic strain as well as the deformation of the PS-domains are confirmed as for the bcc-lattice structure factor. The PS volume fraction can again be calculated to $\phi_{PS} = \eta(R_m/R_{HS})^3 = 0.16 \pm 0.02$ in excellent agreement with the chemical characterization. The domain sizes are only slightly smaller than the expected 97 Å calculated from a relationship by Richards[47] and compare to the volume spanned by the end-to-end distance of the elastic chains of 80 Å. The excess intensity at low q, which is clearly of the q^{-4} type is ascribed to void scattering as a third phase which can occur if inclusions are present.[51] This is further confirmed by the significant reduction of this intensity contribution upon deformation (or compression) as small as 20%.

Further insight into details of order or disorder of the microphase domains is lacking but is unimportant for the purpose of this investigation of matrix properties. Though the PY-like analysis is slightly favorable in view of the dilution with homopolymeric species, a clear distinction is not possible.

4.2. SANS. The Unfilled Reference Network. To obtain reliable information on the strain amplification factor, f, that was already introduced in the first section, it is a prerequisite to study the reference network, i.e., the unfilled network, in terms of chain dimensions R_g, microscopic deformation λ at the chain level, and tube diameter d_0. All deviations from these established values in the filled rubbers will then be assigned to the "reinforcement mechanism by fillers". This approach is justified by the proved equivalence of network parameters obtained by swelling analysis and the similar dimensions of mesh and filler particle from SAXS. For undeformed networks the radially averaged intensity follows the random coil Debye function (eq 5 for $\Lambda = 1$), as expected for a bulk-cross-linked melt, yielding a radius of gyration $R_g = 113 \pm 1$ Å. This is in agreement with the molecular volume of the homopolymer as $M_w/\rho = V_w = 106\,000 \pm 10\,000$ cm^3/mol, which is only slightly larger than the GPC and light-scattering results and yields a characteristic ratio of $C_\infty = 5.1$ for PI.[48] In view of the experimental accuracy of calibrating SANS absolutely, the 5% discrepancy is well within the estimated error.

The data, obtained in the strained state, are interpreted in terms of the tube model for polymer networks mentioned above. If the radius of gyration is kept fixed to its isotropic value in the evaluation of the strained samples, the isotropic tube diameter confirmed a value of $d_0 = 42 \pm 1$ Å, in excellent agreement with our earlier

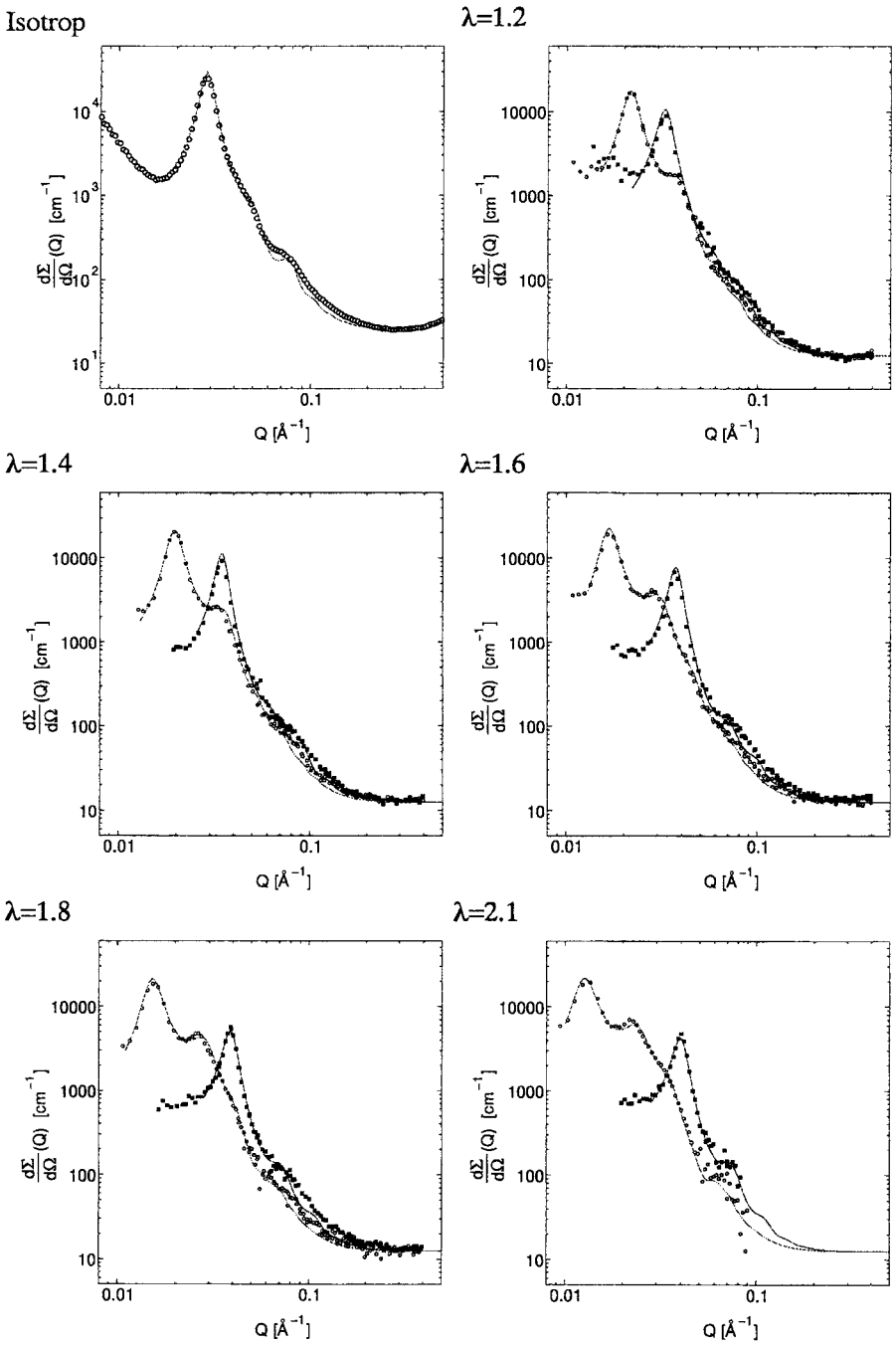

Figure 3. Fit results of the SAXS data using the liquidlike structural premise in the Percus−Yevick approximation. The fits confirm the results of the bcc model. Symbols: circles, parallel direction; squares, perpendicular direction.

findings. The microscopic deformation is reduced in comparison to the affine hypothesis. This is in agreement with other results for networks prepared from cross-linking rather short primary chains. It must be considered as a sensitive function of all chain defects and network fluctuations. A quantitative description of this interplay is presented in a forthcoming study which especially deals with the dependence on primary molecular weights and cross-link densities.[49] For the outcome of the underlying investigation it suffices to relate the deformation in the filled network to the "unfilled deformation".

The Pure PI−PS−PI Triblock Copolymer Melt. The main effort concerning the study of the filled networks was to screen out all coherent scattering contributions of the PS filler domains obeying phase and composition matching conditions. The success of the phase-matching along the triblock copolymer is easily verified in the pure PI−PS−PI melt. The radially averaged data are shown in Figure 4, (lower curve) together with the SAXS curve (upper). A slight matching error results in a remaining peak at $q_{max} = 0.026$ Å^{-1}, identical to the peak position in the SAXS experiment and arises due to the arrangement of the PS domains. The SAXS experiment can be looked at as an hypothetical SANS experiment in which no contrast matching has been applied. The parasitic scattering at low q for neutrons is not q^{-4} and may be due to impurities like wing material, resulting in concentration fluctuation scattering. The SAXS data evidence again void scattering. The contrast for voids is higher for SAXS as for SANS due to the isotopic labeling.[50,51] For a reliable

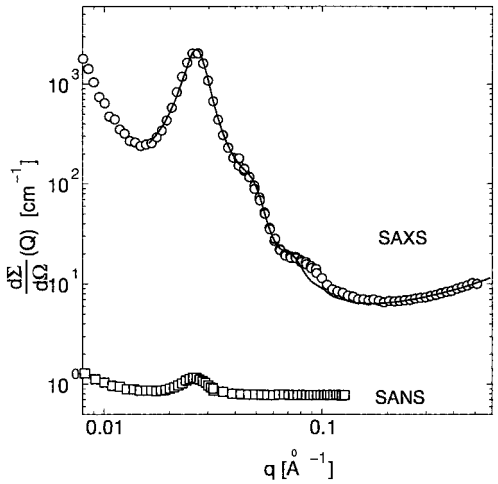

Figure 4. Bottom: Radially averaged SANS data of the pure PI−PS−PI triblock copolymer (×10). The slight mismatch yields a scattering contribution that has to be subtracted in the case of the filled elastomer. Top: SAXS data of pure melt.

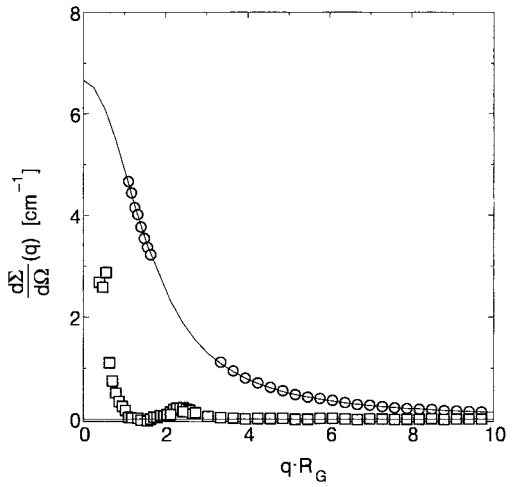

Figure 5. Radially averaged SANS intensity of the undeformed network sample with PS content $\Phi_1 = 0.16$. The data are fitted to a Debye function disregarding the data points influenced by the small deviations from the ideal matching conditions. The residual is shown as open square symbols.

determination of any reinforcement factor from the deformed systems, however, it is essential to determine and subtract the small phase contribution to the scattering.

The Filled Networks. The radially averaged intensity for the Φ_1 sample is shown representatively in Figure 5. For both filled networks the additional scattering contribution due to the small mismatch in the labeling according to eq 4 must be determined by fitting the isotropic data to the Debye function, disregarding the polluted data in the peak region and subtracting the fitted curve. The residual $\delta S(\vec{q},1)$ for the system is included in Figure 5. The data at $qR_g < 1$ now follow the q^{-4} behavior due to void or domain scattering, induced by cross-linking a highly viscous, extremely slow-flowing blend of triblock and homopolymer and are omitted. The radius of gyration was determined to $R_{g1} = 85 \pm 1$ Å for $\Phi_1 = 0.16$ and $R_{g2} = 96 \pm 1$ Å for $\Phi_2 = 0.09$. R_g values for the matrix chains apparently depend quasi-linearly on the overall amount of PS. However, the considerable decrease from 113 to 85 Å with increasing PS content is not accompanied by any visible change of the scattering behavior and may therefore

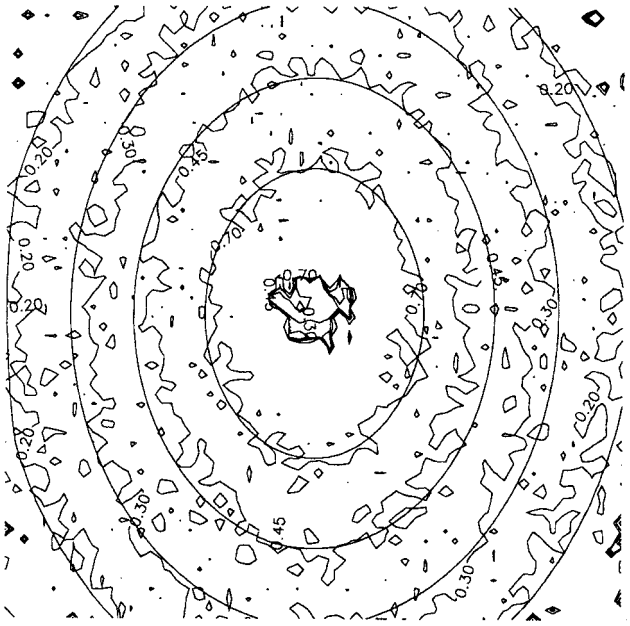

Figure 6. Isointensity contour plot of the two-dimensional SANS data measured from the filled network with $\Phi_1 = 0.16$ and $\lambda = 1.65$ at 10 m detector distance. The solid line is calculated from eq 5 using the parameters of the unfilled reference network. The direction of strain is horizontal.

tentatively be assigned to a partially oriented random walk structure of the configurations of the scattering chains. A similar result was obtained from Monte Carlo simulations for silica-filled PDMS chains.[52] In our case, we believe it to be induced by the preferably radially oriented PI parts of the copolymer micellar chains which penetrate well into the homopolymers. It is very unlikely that it is caused by additional confinement effects. In comparison, if the molecule is part of a folded lamella-structure as is the case, e.g., in partially crystalline materials, the latter radius of gyration is found slightly reduced to the free statistical value.[53]

This residual (neglecting the lowest q region), i.e. the difference $\delta S(\vec{q},1)$ between fit and experimental data is used to correct for the phase scattering of the deformed samples. For $\Lambda \neq 1$, $\delta S(\vec{q},\Lambda)$ is determined taking into account the SAXS result of an affine displacement of the latticelike domains which leads to the transformation

$$\delta S(\vec{q},\Lambda) = \delta S(\Lambda^{-1}\vec{q},1) \qquad (6)$$

The method was tested thoroughly along both principal axes and then expanded in the 2D plane. Due to the two different detector settings, mainly the longest distance is polluted whereas only minor effects for the shorter detector-to-sample distance are expected. Figure 6 shows corrected scattering intensities in a 2D contour plot for the small q interval ($-3 < qR_g < +3$) monitored at a detector distance of 10 m for the representative case of $\Phi_1 = 0.16$ and a macroscopic deformation of $\lambda = 1.65$. The theoretical curve is calculated from the tube model (eq 5) based on the parameters of the unfilled reference sample without introducing an overstrain factor. The perpendicular direction, i.e., the long axis of the ellipsoidal data, fits the experimental data fairly well whereas along the strain direction, i.e., the short axis, the intensity decreases faster than the theory predicts. The experimental anisotropy is therefore larger than the theoretical one. Theory and experiment disagree con-

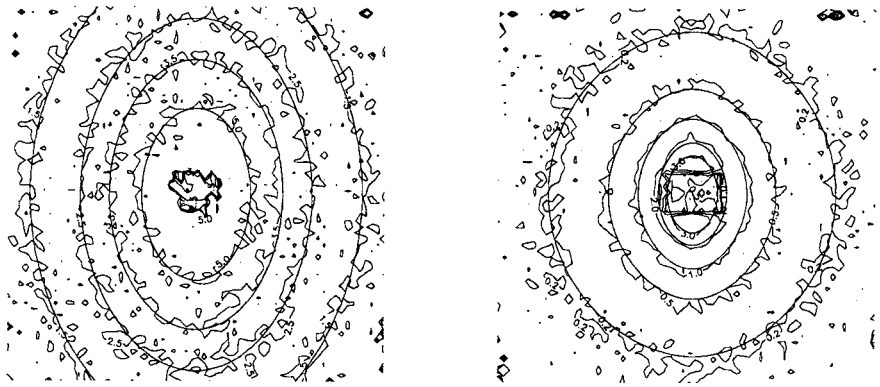

Figure 7. Isointensity contour plot of the two-dimensional SANS data measured from the filled network with $\Phi_1 = 0.16$ at $\lambda = 1.65$ for both detector distances. The solid line is calculated from eq 5 using the parameters of the unfilled reference network, corrected by the overstrain factor $f = 1.89$

Table 2

Φ	λ	f	Φ	λ	f
0.09	1.20	1.36	0.16	1.40	1.84
	1.40	1.37		1.55	1.88
	1.65	1.38		1.70	1.89
				1.90	1.91

siderably in the intermediate to large q region. If the microscopic overstrain factor f, given in eq 2, is introduced into eq 5, using the transformation of λ to $\bar{\lambda}$, the average microscopic overstrain factor f becomes the only relevant parameter to be optimized further. Since the network parameters are similar, all chain parameters except for the strain amplification can be estimated from the unfilled case. The tube diameter proved stable in a trial refinement and was fixed further on. In our representative example a value of $f = 1.89$ was determined, which gives an excellent fit for the whole q range studied in the 2d plane and both principal axes; this is shown in Figure 7 for the low q range (left) and high q range (right). The model as such therefore represents the first direct microscopic proof of a matrix chain overstrain in this composite model for filled elastomers. To determine whether f also depends on strain—unlike eq 3—all anisotropic spectra were evaluated in the same way. The results are summarized in Table 2.

5. Discussion

Figure 8 presents the experimental values for f vs the volume fraction of filler for two different deformation ratios, 1.4 and 1.7. The lower solid line corresponds to the Padé approximation according to eq 3. The experimental overstrain factors are underestimated if the volume fraction of filler is entirely given by the chemical composition of the triblock copolymer. It is, however, common empirical practice [19] to express deviations in the description of mechanical data in terms of effective volume fractions, Φ_{eff}, parametrized according to $\Phi_{\text{eff}} = \Phi(1 + \delta(\lambda))$. The latter correction was substituted for Φ in the Padé formula and $1 + \delta(\lambda)$ fitted as a function of the macroscopic sample deformation to yield both upper curves of Figure 8. The dependence of $1 + \delta(\lambda)$ as a function of the macroscopic sample deformation is shown in Figure 9 for both volume fractions. The correlation is linear and is described as $1 + \delta(\lambda) = 1.1 + 0.12\lambda$ or equivalently $1.22 + 0.12(\lambda - 1)$. This is very close to the experimental variation of the domain radius from SAXS, found to be $R = R_0(1 + 0.11\lambda)$ where R_0 is the isotropic domain size and is well in line with recent theoretical work by Huber[15] on reinforcement by fractal

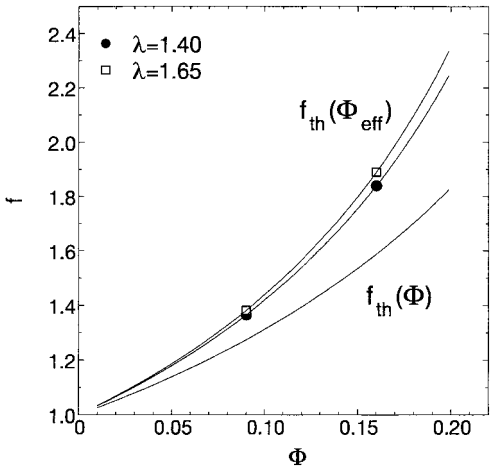

Figure 8. Variation of the microscopic overstrain factors f as a function of the filler volume fraction Φ and two strains. The lower solid line is the behavior predicted from continuum mechanics according to the Padé approximation in eq 3. The upper curves are obtained after substitution of an effective filler volume fraction Φ_{eff} for Φ in eq 3.

aggregates. There, the strain amplification factor f is predicted to scale according to a power law R^{α} where α depends on the fractal dimensions of the aggregates and surface and simply reduces to 1 in our case. This linear dependence on R is confirmed by the first observation.

Considering the existence of a diffuse PS−PI boundary layer around the PS domains of which a thickness $\sigma = 4 \pm 3$ Å could be extracted from the synchrotron data, an estimate for the increase in volume would yield $1 + \delta(\lambda \rightarrow 1) = (R_{\text{PS}} + \sigma)^3 / R_{\text{PS}}^3 = 1.14 \pm 0.15$. The agreement with the correction factor of the effective volume fraction from an extrapolation of the SANS data to the isotropic state, i.e. $1 + \delta(\lambda \rightarrow 1) \approx 1.22$, is good and confirms the presence of a more or less hard transition layer between filler and rubbery matrix indirectly also by SANS. This firmly bound mixed-phase layer, which can be expected to be the primary reason for the increased effective volume here, is of a somewhat different nature than in real filled systems where mainly absorption is the key process but results in the same Φ dependence.

The (rough) assumption of homogeneous strain throughout the whole matrix, for which eq 1 was derived strictly, implies at the same time a homogeneous stress distribution at any point in the sample. Clearly, the strain may depend on the position relative to the filler particles, where even isotropic states may be possible.

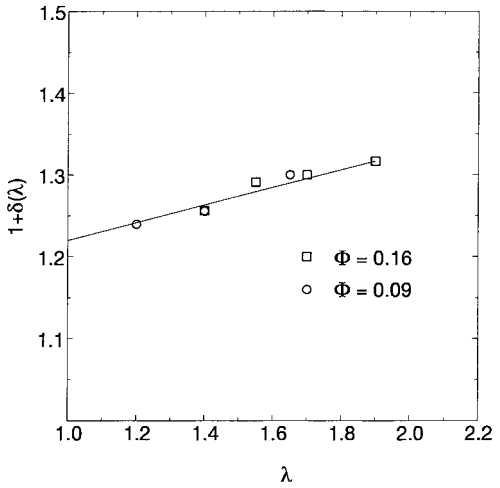

Figure 9. Variation of $1 + \delta(\lambda)$ with extension ratio. The solid line is a linear fit according to $1 + \delta(\lambda) = 1.1 + 0.12\lambda$. The correlation with the deformation of the filler is excellent.

Scattering data for the sample with $\Phi_1 = 0.16$ at the highest available macroscopic extension ratio $\lambda = 1.9$ (not shown because of too bad statistics) reveal a slight but systematic deviation of the fit curves in an off-axis q region, close to the isotropic angle,[28] if the residual 2d-scattering intensities in a relative-difference plot, $(I_{theo} - I_{exp})/I_{theo}$, are inspected. The strain amplification concept seems to be restricted to the lower linear elasticity regime.

The individual moduli are about 0.5 MPa for the soft PI matrix and 2 GPa for the glassy PS, and consequently a fulfillment of the assumption of no deformation of the filler domains must be expected. The experimental radii from the SAXS analysis, however, are consistently different upon strain. For $\lambda = 1.9$, the overstrain in the matrix $\epsilon_{PI} = \Lambda - 1$ yields 1.72 and is $\epsilon_{PS} = [(R_{m,\lambda}/R_m) - 1] = 0.11$ for the fillers. Their ratio is about 16 and is much less than expected from the ratio of moduli, 2000/0.5 = 4000. In the perpendicular direction, the ratio even reduces to about 4. The discrepancy for both directions may be attributed to different sensitivities to strain. Perpendicularly, the network is compressed, thereby possibly forcing apart microdomains of PS in the parallel direction. A reorganization along this direction would bring the same effect. The observed weakness of the hard domains may have its roots in the inclusion of soft segments inside the glassy domains. As all samples showed qualitatively 100% recoverable strain immediately after strain release, no so-called strain-induced-plastic-to-rubber transition seems to have occurred. This was found for thermoplastic elastomers of the PS−PI−PS type,[54,55] at considerably higher strains. Therefore, the inclusion hypothesis is moreprobable due to the micellar-like structure of the microphase separation.

With respect to the rather limited statistics, the observation concerning the inhomogeneity of the strain encourages further experiments at higher strains and filler fractions. Our data do not allow a more refined statement to this point of interpretation. Nevertheless, the strain amplification concept, which is a recognized cause of reinforcement,[1] could be proven unambiguously.

6. Conclusion

In this work, we have studied the phenomenon of rubber reinforcement on a model composite system simulating the filler by microphase-separated spherical PS domains. All length scales of interest as well as sizes of the domains themselves are available. By judiciously matching the scattering properties of the filler component by that of the matrix, we studied the effect of the reinforcement on the matrix chains by neutron scattering, while on the same samples the response of the filler due to the different scattering contrast could be studied by synchrotron radiation.

The SAXS experiment yielded a mean filler radius of about 84 Å, and an affine correlation of the filler displacement with macroscopic sample strain was found. The variation of the domain radius with the strain indicated that the PS spheres are softer than expected, which may be attributed to the presence of some polyisoprene chains within the PS domains reducing the density of the micelle-like core.

The SANS experiments were evaluated using an extension of the tube model for randomly cross-linked networks and the molecular parameters derived were in good agreement with the values expected for the unfilled case. The reinforcement factor is dependent on the filler concentration according to the overstrain picture and varies slightly with strain. The data were fitted to a very high degree of accuracy with the assumption of an homogeneous overstrain in the matrix, but first signs of a breakdown of this crude treatment have shown up at higher strains.

This work reports for the first time a direct experimental determination of the overstrain factor which has to be considered in reviewing semimicroscopic theories of the rubber reinforcement with real filler materials. This work encouraged the analysis of contrast-matched silica-filled systems, which is currently in progress.

Acknowledgment. The authors thank the Institute Laue Langevin, Grenoble, France, for the use of the beamtime. M. Hintzen is gratefully acknowledged for the sample preparation and characterization. Discussions with Dr. G. Heinrich, Continental AG, Hannover, Germany, are appreciated.

References and Notes

(1) Dannenberg, E. M. *Rubber Chem. Technol.* **1975**, *48*, 410.
(2) Donnet, J.-B. *Carbon Black*; M. Dekker: New York, Basel, Switzerland, and Hong Kong, 1993.
(3) Einstein, A. *Ann. Phys.* **1911**, *34*, 591.
(4) Smallwood, H. M. *J. Appl. Phys.* **1944**, *15*, 758.
(5) Inoue, T.; Moritani, M.; Hashimoto, T.; Kawai, H. *Macromolecules* **1971**, *4*, 500.
(6) Donnet, J.; Vidal, A. *Prog. Colloid Polym. Sci.* **1987**, *75*, 201−212.
(7) Guth, E.; Gold, O. *Phys. Rev.* **1938**, *53*, 322.
(8) Richards, R. W.; Welsh, G. *Eur. Polym. J.* **1995**, *31*, 1197.
(9) Edwards, D. C. *J. Mater. Sci.* **1990**, *25*, 4175−4185.
(10) Benson, R.; Lee, M.; Gummit, D. *Nanostruct. Mater.* **1995**, *6*, 83−91.
(11) Ihon, M.; Metz, R.; Freed, K. *J. Stat. Phys.* **1988**, *82*, 1325.
(12) Heinrich, G.; Vilgis, T. *Kautsch. Gummi Kunstst.* **1992**, *45*, 1006.
(13) Huber, G. Ph.D. Thesis, University of Mainz, Germany, 1997.
(14) Castaing, J.; Allain, C.; Auroy, P.; Pouchelon, L.; Auvray, A. *Europhys. Lett.* **1996**, *36*, 153.
(15) Huber, G.; Vilgis, T. *Kautsch. Gummi Kunstst.* **1999**, *2*, 102.
(16) Edwards, S. F.; Vilgis, T. A. *Rep. Prog. Phys.* **1988**, *51*, 243−297.
(17) Heinrich, G.; Straube, E.; Helmis, G. *Adv. Polym. Sci.* **1988**, *85*, 33−87.
(18) Nakajima, N.; Scobbo, J. *Rubber Chem. Technol.* **1988**, *61*, 137−148.
(19) Wolff, S.; Donnet, J.-B. *GAK-Gummi Fasern Kunstst.* **1990**, *43*, 670.

(20) Eggers, H.; Schummer, P. *Rubber Chem. Technol.* **1996**, *69*, 253−265.
(21) Mullins, L.; Tobin, N. R. *Rubber Chem. Technol.* **1966**, *39*, 799.
(22) Bueche, F. *J. Appl. Polym. Sci.* **1961**, *15*, 271.
(23) Kotani, T.; Sternstein, S. S. In *Polymer Networks*; Chompff, A. J., Ed.; Plenum: New York, 1971.
(24) Ong, C. S. M.; Stein, R. S. *J. Polym. Sci., Phys.* **1974**, *12*, 1899.
(25) Ullman, R. *Macromolecules* **1982**, *15*, 1395.
(26) Kloczkowski, A.; Mark, J. E.; Erman, B. *Comput. Polym. Sci.* **1992**, *2*, 8.
(27) Straube, E.; Urban, V.; Pyckhout-Hintzen, W.; Richter, D. *Macromolecules* **1994**, *27*, 7681.
(28) Straube, E.; Urban, V.; Pyckhout-Hintzen, W.; Richter, D.; Glinka, C. J. *Phys. Rev. Lett.* **1995**, *74*, 4464.
(29) Read, D. J.; McLeish, T. C. B. *Phys. Rev. Lett.* **1997**, *79*, 87.
(30) Bastide, J.; Herz, J.; Boue, F. *J. Phys.* **1985**, *46*, 1967.
(31) Higgs, P.; Ball, R. *J. Phys. Fr.* **1988**, *49*, 1785.
(32) des Cloizeaux, J. *J. Phys. Fr.* **1993**, *4*, 539.
(33) Westermann, S.; Urban, V.; Pyckhout-Hintzen, W.; Richter, D.; Straube, E. *Macromolecules* **1996**, *29*, 6165−6174.
(34) Christensen, R. M. *Mechanics of Composite Materials*; Wiley: New York, Chichester, England, Brisbane, Australia, and Toronto, Canada, 1979.
(35) H.-S. Chen, A. Acrivos, *Int. J. Solids Struct.* **1978**, *14*, 331.
(36) Heinrich, G.; Vilgis, T. *Macromolecules* **1993**, *26*, 1109−1119.
(37) Quan, X.; Gancarz, I.; Koberstein, J. T. *J. Polym. Sci., Part B: Polym. Phys.* **1987**, *25*, 641.
(38) Quan, X.; Koberstein, J. T. *J. Polym. Sci., Part B: Polym. Phys.* **1987**, *25*, 1381.
(39) Benmouna, M.; Benoit, H. *J. Polym. Sci. Polym. Phys. Ed.* **1983**, *21*, 1227.
(40) Kaliske, M.; Heinrich, G. *Comput. Theor. Polym. Sci.* **1997**, *7*, 227−241.
(41) Kinning, D. J.; Thomas, E. L. *Macromolecules* **1984**, *17*, 1712.
(42) Leibler, L. *Macromolecules* **1980**, *13*, 1602.
(43) Schwab, M.; Stuehn, B. *Phys. Rev. Lett.* **1996**, *76*, 924.
(44) Schwab, M.; Stuehn, B. *J. Mol. Str.* **1996**, *383*, 57.
(45) Menge, H. Private communication.
(46) Hoover, W. G.; Ree, F. H. *J. Chem. Phys.* **1968**, *49*, 3609.
(47) Richards, R. W.; Thomason, J. L. *Polymer* **1983**, *24*, 275−278.
(48) Hadjichristidis, N.; Xu, Z.; Fetters, L. J.; Roovers, J. *J. Polym. Sci. Polym. Phys. Ed.* **1982**, *20*, 743.
(49) Pyckhout-Hintzen, W.; Westermann, S.; Botti, A.; Urban, V.; Richter, D.; Straube, E. *ACS Rubber Divison 155th Spring Meeting, Chicago, April 13−16, 1999*; ACS Rubber Division: 1999.
(50) Wignall, G. D.; Farras, N. R.; Morris, S. *J. Mater. Sci.* **1990**, *25*, 69.
(51) Marr, D. W.; Wartenberg, M.; Schwartz, K. B.; Agamalian, M. M.; Wignall, G. *Macromolecules* **1997**, *30*, 2120.
(52) Yuan, Q.; Kloczkowski, A.; Mark, J.; Sharaf, M. *J. Polym. Sci., Polym. Phys. Ed.* **1996**, *34*, 1647.
(53) Fischer, E.; Hahn, K.; Kugler, J.; Struth, U.; Born, R.; Stamm, M. *J. Polym. Sci., Polym. Phys. Ed.* **1984**, *22*, 1481−1513.
(54) Pakula, T.; Saijo, K.; Kawai, H.; Hashimoto, T. *Macromolecules* **1985**, *18*, 1294.
(55) Pakula, T.; Saijo, K.; Hashimoto, T. *Macromolecules* **1985**, *18*, 2037.

MA990112E